

BNL--41948

DE89 005663

Search for Flavor Changing Neutral Currents
 $K_L^0 \rightarrow \mu^\pm e^\mp$, e^+e^- and $\pi^0 e^+e^-$

W.M. Morse, E. Jastrzembski, R.C. Larsen, and L.B. Leipuner
 Department of Physics
 Brookhaven National Laboratory, Upton, NY 11973

H.B. Greenlee, H. Kasha, E.B. Mannelli, M. Mannelli,
 K.E. Ohl, S.F. Schaffner, and M.P. Schmidt
 Department of Physics
 Yale University, New Haven, CT 06511

ABSTRACT

We report on a search for the flavor-changing neutral-current decays
 $K_L^0 \rightarrow \pi^0 e^+e^-$, $K_L^0 \rightarrow e^+e^-$ and $K_L^0 \rightarrow \mu^\pm e^\mp$. Limits obtained for
 these processes are $BR(K_L^0 \rightarrow \pi^0 e^+e^-) < 3.2 \times 10^{-7}$, $BR(K_L^0 \rightarrow e^+e^-)$
 $< 1.2 \times 10^{-9}$, $BR(K_L^0 \rightarrow \mu^\pm e^\mp) < 1.9 \times 10^{-9}$.

JAN 17 1989

DISCLAIMER

This report was prepared as an account of work sponsored by an agency of the United States Government. Neither the United States Government nor any agency thereof, nor any of their employees, makes any warranty, express or implied, or assumes any legal liability or responsibility for the accuracy, completeness, or usefulness of any information, apparatus, product, or process disclosed, or represents that its use would not infringe privately owned rights. Reference herein to any specific commercial product, process, or service by trade name, trademark, manufacturer, or otherwise does not necessarily constitute or imply its endorsement, recommendation, or favoring by the United States Government or any agency thereof. The views and opinions of authors expressed herein do not necessarily state or reflect those of the United States Government or any agency thereof.

MASTER

REPRODUCTION OF THIS DOCUMENT IS UNLIMITED

The decays $K_L^0 \rightarrow \pi^0 e^+ e^-$ and $K_L^0 \rightarrow e^+ e^-$ occur as a consequence of strangeness changing neutral currents and are highly suppressed in the Standard Model. The decay $K_L^0 \rightarrow \mu^\pm e^\mp$ is forbidden by lepton generation number conservation. The decay $K_L^0 \rightarrow \pi^0 e^+ e^-$ through one photon exchange is a CP violating process. Decays to $\pi^0 e^+ e^-$ can proceed through vector or scalar currents, while decays to $e^+ e^-$ are mediated by axial vector or pseudoscalar currents.

The decay $K^+ \rightarrow \pi^+ e^+ e^-$ is known to occur¹ with a branching ratio of $(2.7 \pm 0.5) \times 10^{-7}$. Theoretical estimates² of the decay rate for the CP-conserving decay $K_S^0 \rightarrow \pi^0 e^+ e^-$ range from one-tenth of the rate for $K^+ \rightarrow \pi^+ e^+ e^-$ to 2.5 times that rate while the rate for similar $K_L^0 \rightarrow \pi^0 e^+ e^-$ decays is expected to be reduced by the factor ϵ^2 in the absence of any direct CP-violating amplitude. Theoretical estimates² of the transition $K_L^0 \rightarrow \pi^0 e^+ e^-$ range from $2 \cdot 10^{-12}$ to $3 \cdot 10^{-11}$. The branching ratio for a CP-conserving decay transition through two virtual photons is expected to be below 10^{-11} . The decay $K_L^0 \rightarrow \pi^0 e^+ e^-$ is then an excellent window to search for light scalar particles that couple to $e^+ e^-$. In such searches the K_L^0 branching ratio is expected to be about 8.4 times the K^+ branching ratio to π^+ and a light scalar.³ Furthermore, some non-standard models of CP-invariance violation⁴ predict branching ratios higher than $3 \cdot 10^{-11}$. The present 90% confidence level limit⁵ for this decay is $BR(K_L^0 \rightarrow \pi^0 e^+ e^-) < 2.3 \cdot 10^{-6}$.

The decay $K_L^0 \rightarrow e^+ e^-$ is suppressed in the standard model with respect to the observed rare decay $K_L^0 \rightarrow \mu^+ \mu^-$ because of the small value of m_e/m_K . The unitarity limit⁶ for $K_L^0 \rightarrow e^+ e^-$ is $BR(K_L^0 \rightarrow e^+ e^-) > 2.5 \times 10^{-12}$. This decay is then particularly sensitive to new interactions proceeding through pseudoscalar currents.

The present limit⁷ is $BR(K_L^0 \rightarrow e^+e^-) < 4.5 \times 10^{-9}$. The unitarity limit for $K_L^0 \rightarrow \mu^+\mu^-$ is $BR(K_L^0 \rightarrow \mu^+\mu^-) > (7.0 \pm 0.3) \times 10^{-9}$.

The data for this study comes from an experiment conducted at the Brookhaven AGS. The diagram of Fig. 1 shows a schematic representation of the experimental apparatus. A neutral beam, produced in the forward direction by the interaction of 24 GeV protons on a copper target, passed 7.47 m through vacuum and an 8 Tesla-meter clearing field, into a 2.87 m long decay region. Gamma rays from the target were attenuated by a 2.5 cm lead beam plug. The momenta of the charged particles from K-decays were then determined by a magnetic spectrometer made up of two upstream sets of mini-drift chambers with maximum drift distance of 3 mm (labeled A and B), a magnet with a field integral of $\Delta p_t = 220 \text{ MeV}/c$, and two downstream minidrift chambers (labeled C and D). The geometrical acceptance was 3.5% for $K_L^0 \rightarrow e^+e^-$, 3.7% for $K_L^0 \rightarrow \mu^+\mu^-$, and .024% for $K_L^0 \rightarrow \pi^0 e^+e^-$.

The electrons were identified by a 3 m. long atmospheric pressure hydrogen Cerenkov counter. Pions with energies less than 8 GeV were not registered by the Cerenkov counter. The electron energies were measured in a lead glass array consisting of 244 blocks of Schott F2 glass with dimensions of 6.35 cm \times 6.35 cm \times 46 cm. The glass blocks were arranged in a 1 m \times 1 m array with a central 12.7 cm \times 38 cm hole to pass the neutral beam. The blocks were optically isolated with 50 μ m. aluminized mylar. The photomultiplier bases employed a variable high voltage power supply which was connected to the photocathode and a fixed high voltage power supply which was connected to the ninth dynode of a 12 stage tube. This reduced variations in gain as a function of beam intensity. Custom built ADC modules were used to integrate the charge from the lead glass

counters. The signals were integrated for 120 nsec. An "in-time bit" was set if a leading edge above an effective threshold of 500 MeV occurred within ± 5 nsec. of the trigger. The pedestals were recorded at random times during the beam spill. The ADC modules subtracted the pedestals and only read out channels above a threshold of 70 MeV. We accepted typically 8×10^{11} protons per AGS pulse, which generated approximately 10^7 counts/m²/sec. in the detector. The data was collected from February to May, 1988.

Four trigger types were collected: μe , ee , $\mu\mu$, and $\pi\pi$. All triggers required drift chamber hits on the left and the right of the neutral beam in the bend view drift chambers. As defined by the hardware trigger, electrons were particles that triggered the Cerenkov counter and deposited at least 1.2 GeV in the glass array; particles which penetrated a 1.05 m steel filter were defined as muons; those particles that did not activate the μ or e triggers but penetrated the glass array, but not the steel filter were classified as pions. The $\pi\pi$ trigger was prescaled by a factor of 128. A Fastbus processor aborted events which did not have A, B, and C drift chamber hits compatible with two tracks in the bend view which originated in the decay volume. However, no on-line cuts were made to reject three body decays. The data acquisition livetime was typically 90%.

The ee triggers largely derive from K_{e3} decays such that the pion energy is above the Cerenkov threshold while the μe triggers were generated for the most part from K_{e3} decays where the pion either punches through the steel filter or decays in flight to a muon that passes through the filter. The energy deposited in the lead glass for electrons from the K_{e3} decays was compared with the momentum determined

in the magnetic spectrometer to provide an accurate off-line calibration of the lead glass. The lead glass energy resolution was determined to be $\sigma/E = 11\%/\sqrt{E}$ (E in GeV). The resolution was measured to be $7\%/\sqrt{E}$ when the glass was purchased. We attribute the difference to radiation damage. Most of the blocks appear noticeably yellow compared to new lead glass. The lead glass position resolution was measured to be ± 6 mm. The efficiency of the Cerenkov counter was 93% for inbending electrons and 83% for outbending electrons.

Measurements of the decays $K^0_L \rightarrow \pi^0 \pi^+ \pi^-$ serve to determine a normalization for the $K^0_L \rightarrow \pi^0 e^+ e^-$ decays as well as providing a useful measure of mass resolutions for the topologically similar $\pi^0 e^+ e^-$ final states. The charged tracks were required to pass requirements on track quality and distance of closest approach at the vertex. Events were rejected if there were more than two tracks⁸ pointing to the vertex. All events were required to have at least two gamma clusters in the lead glass besides the two clusters associated with the charged tracks. The gamma clusters were required to be in a fiducial region which excluded the blocks around the beam hole. Only those gamma clusters were selected such that greater than 1 GeV was deposited in the cluster and the intime bit was activated. Figure 2a shows a histogram of the measured $\gamma\gamma$ invariant mass for such events. For events with more than two gamma clusters, all $\gamma\gamma$ invariant mass combinations are shown. Only events with exactly one $\gamma\gamma$ combination within $30 \text{ MeV}/c^2$ of the π^0 mass were selected. If the invariant mass of the $\gamma\gamma$ set within $30 \text{ MeV}/c^2$ of the π^0 mass is constrained to the π^0 mass, the K-mass is determined to an

uncertainty of $\sigma = 3.7 \text{ MeV}/c^2$. With this result as a normalization, the mass uncertainty for the final state $\pi^0 e^+ e^-$ was calculated to be $\sigma = 4.4 \text{ MeV}/c^2$.

The events are also constrained by the requirement that they point back to the target. For otherwise acceptable $\pi^0 \pi^+ \pi^-$ events, $\sigma(\theta) \approx 1 \text{ mrad}$, where θ is the angle between the line from target to the decay point and the total momentum vector. We require $\pi^+ \pi^- \pi^0$ events to be within $12.5 \text{ MeV}/c^2$ of the K mass and have $\theta^2 < 10 \text{ mrad}^2$. The $\pi^+ \pi^- \pi^0$ effective mass and θ^2 distributions are shown in Figs. 2b and 2c respectively. These distributions are especially clean. No corrections have been made for backgrounds under the peaks.

The resolution for $e^+ e^-$ decays is determined from the kinematically similar $K_L^0 \rightarrow \pi^+ \pi^-$ sample. Figure 3a shows the $\pi^+ \pi^-$ effective mass for inbending events. The distribution in θ^2 is shown in Fig. 3b. The mass resolution is $2.3 \text{ MeV}/c^2$ for inbending events and $4.0 \text{ MeV}/c^2$ for outbending events. The resolution in θ is 0.33 mrad for both event samples. We require $\pi^+ \pi^-$ events to be within three sigma of the K mass and have $\theta^2 < 1.5 \text{ mrad}^2$. However, radiative effects⁹ are important for decays to $\pi^0 e^+ e^-$ and $e^+ e^-$. For example 15% of $K_L^0 \rightarrow e^+ e^-$ decays will have an $e^+ e^-$ effective mass more than $20 \text{ MeV}/c^2$ below the K mass.

Electron identification was established off-line using the lead glass information. The momentum measured in the magnetic spectrometer was required to be close to the energy measured in the lead glass array. The distribution in E/p for K_{e3} events from μe and ee triggers is shown in Fig. 4. The tail at large E/p is due to accidental overlap at high rates and is not seen in low intensity runs. We require $E/p > 0.75$ for electrons. Furthermore, the electron momentum was required to be below

the pion Cerenkov threshold of 8 GeV/c for the $\pi^0 e^+ e^-$ search and the $e^+ e^-$ effective mass was required to be greater than 150 MeV/c² to reject π^0 Dalitz decays. The momentum asymmetry $A = (P_{\max} - P_{\min}) / (P_{\max} + P_{\min})$ was required to be less than 0.6 for the $e^+ e^-$ search. From Monte Carlo calculations it was determined that > 97% of $e^+ e^-$ decays satisfy the momentum asymmetry constraint.

Figure 5 shows a plot of the $e^+ e^-$ effective mass vs. θ^2 for $e^+ e^-$ triggers which satisfy the above criteria. We find no events consistent with $K^0_L \rightarrow e^+ e^-$. The nearest event with an acceptable θ^2 is 25 MeV/c² below the K mass. The events below the K mass are consistent with Monte Carlo calculations of K_{e3} events with the pion misidentified as an electron. The normalization for $K^0_L \rightarrow e^+ e^-$ is determined by the number of observed $K^0_L \rightarrow \pi^+ \pi^-$ decays. A correction of 15% was applied to account for background contributions in mass and θ^2 . The background subtracted data was then fit as a function of K energy and decay position to determine the K^0_S contamination. It was determined that effectively 78% of the $\pi\pi$ decays were due to K^0_L . Then using the known $\pi\pi$ branching ratio and the ratio of ee to $\pi\pi$ acceptances as determined by Monte Carlo calculations, the single event sensitivity to $K^0_L \rightarrow e^+ e^-$ was determined to be 7.2×10^{-10} . We then determine the 90% confidence level limit $BR(K^0_L \rightarrow e^+ e^-) < 1.6 \times 10^{-9}$. Combining this result with our 1987 limit⁷ gives a final limit $BR(K^0_L \rightarrow e^+ e^-) < 1.2 \times 10^{-9}$.

A plot of $m(\pi^0 e^+ e^-)$ vs. θ^2 is shown in Fig. 6. There were no $\pi^0 e^+ e^-$ candidate events consistent with pointing back to the target. Only one of the events in the plot survives a more stringent lead glass cut of $.85 < E/p < 1.25$. The acceptance of the experiment to $\pi^0 e^+ e^-$ was calculated by Monte Carlo methods as a function of the $e^+ e^-$ effective mass. The

dileptons were generated isotropically in their rest frame. The normalization for $\pi^0 e^+ e^-$ was determined through an accounting of the topologically similar decay $K^0_L \rightarrow \pi^0 \pi^+ \pi^-$. The 90% confidence level limits on $K^0_L \rightarrow \pi^0 e^+ e^-$ are shown as a function of $e^+ e^-$ effective mass in Fig. 7. For a population of events distributed uniformly in the Dalitz plot, the 90% confidence limit is $BR(K^0_L \rightarrow \pi^0 e^+ e^-) < 3.6 \times 10^{-7}$.

During an earlier run in 1987, approximately one third of the data was taken without on-line cuts to reject 3 body K decays. The ADC in-time bit was not implemented for that run. There was one event consistent with pointing back to the target ($\theta^2 = 0.7 \times 10^{-6}$). However, the $\pi^0 e^+ e^-$ effective mass was only 481 MeV/c². Furthermore, this event, which had additional hits in the first two drift chambers, was consistent with the decay $K^0_L \rightarrow \pi^0 \pi^0$ with both π^0 's undergoing Dalitz decay¹⁰. A cut was applied to the data to reject events with extra track stubs⁸. This cut rejected about 1.5% of the normalization events. After applying this cut, there were no events left in the region shown in Fig. 6. Combining the results from both runs, the 90% confidence level limit is $BR(K^0_L \rightarrow \pi^0 e^+ e^-) < 3.2 \times 10^{-7}$.

The constraints of kinematic reconstruction are especially important in searches for $K^0_L \rightarrow \mu^+ \mu^-$ and $\mu^\pm e^\mp$ to discriminate against backgrounds from $K^0_L \rightarrow \pi \mu \nu$ and $\pi e \nu$ with the pion decaying to or being misidentified as a muon. For example, if the neutrino is produced with very little energy in the K rest frame and the muon from π decay is directed along the π trajectory, the dilepton effective mass equals 489 MeV/c². However, in this case the transverse momentum with respect to the target for nearly transverse K decays will be unbalanced by approximately 9 MeV/c. If the π decays so as to affect the momentum

measurement, the measured dilepton mass can even exceed the K mass. Then, however, the event will not have an acceptable θ^2 . We expect similar background distributions in the $\mu^\pm e^\mp$ and $\mu^+\mu^-$ searches.

The decay $K_L^0 \rightarrow \mu^+\mu^-$ served to verify our estimation of the sensitivity of the experiment. Various cuts were applied to reduce backgrounds. The momentum asymmetry $A = (P_{\max} - P_{\min}) / (P_{\max} + P_{\min})$ was required to be less than 0.45. 93% of the $\pi^+\pi^-$ events pass this cut. Monte Carlo calculations show that 95% of $\mu^\pm e^\mp$ decays would pass this cut. Muons were required to penetrate at least 1.05m of steel to satisfy the trigger. Furthermore, if the muon stopped in the range stack, the energy obtained from the muon range was required to be at least 70% of the momentum as measured in the magnetic spectrometer. From our study of $K_{\mu 3}$ events, only 3% of muons fail this cut. Only inbending events were used in this analysis.

A scatter plot of $\mu^+\mu^-$ effective mass vs. θ^2 is shown in Fig. 8a. The distribution of $m(\mu^+\mu^-)$ for events which point back to the target to within 1.5 mrad^2 is shown in Fig. 8b. There is a clear peak around the K mass. All eight events are within 1.8σ of the K mass. As stated above, we expect similar background distributions in the μe and $\mu\mu$ data. Since there are no events in the fiducial region in the μe sample (see below), we subtract no background from the number of $\mu\mu$ events in the fiducial region. The sensitivity of the experiment to the decay $K_L^0 \rightarrow \mu^+\mu^-$ was determined through an accounting of the kinematically similar decay $K_L^0 \rightarrow \pi^+\pi^-$. Corrections were made for the efficiency of the muon trigger counters. Using the known $\pi\pi$ branching ratio, it was determined that the single event sensitivity to $K_L^0 \rightarrow \mu^+\mu^-$ was 1.3×10^{-9} . Using the single event sensitivity and the Particle Data Group world average

$BR(K_L^0 \rightarrow \mu^+ \mu^-) = (9.1 \pm 1.9) \times 10^{-9}$, we would expect to observe 7.0 events, in good agreement with the eight events in the fiducial region.

The same kinematic and muon identification requirements were made on the μe triggers. Additional requirements were made on the electron track. The electron momentum was required to be less than the pion Cerenkov threshold of 8 GeV/c. Furthermore, the energy as measured in the lead glass divided by the momentum measured in the magnetic spectrometer was required to be greater than 0.75. 96% of electrons satisfy this requirement. A scatter plot of $\mu^\pm e^\mp$ effective mass vs. θ^2 is shown in Fig. 9a. The distribution of $m(\mu e)$ for events which point back to the target to within 1.5 mrad^2 is shown in Fig. 9b. There are no events close to the K mass. The closest event had an effective mass of $489.3 \text{ MeV}/c^2$. This is 3.7σ below the K mass. We then find no events consistent with the decay $K_L^0 \rightarrow \mu e$. The single event sensitivity to the decay $K_L^0 \rightarrow \mu e$ was determined to be 1.1×10^{-9} . The 90% confidence level limit is then $BR(K_L^0 \rightarrow \mu e) < 2.6 \times 10^{-9}$. Combining this result with our previous limit⁷ gives a final result $BR(K_L^0 \rightarrow \mu e) < 1.9 \times 10^{-9}$. This limit places constraints on models with exotic gauge bosons: assuming the boson couples to μe and sd with the universal weak coupling constant, the mass of such a boson is related to the K_L^0 branching ratio by $BR(K_L^0 \rightarrow \mu e) \approx 2.5 \times 10^{-3} (M_X/1 \text{ TeV})^{-4}$. Our result thus requires $M_X > 34 \text{ TeV}$.

We thank the Brookhaven AGS accelerator department staff for their support. We gratefully acknowledge the timely loan of lead glass blocks from M. Kreisler and colleagues at the University of Massachusetts, Amherst, and photomultiplier tubes from Brookhaven National Laboratory

experiment No. 734. We gratefully acknowledge the contributions of R.K. Adair who worked on the earlier stages of the experiment. We also wish to thank Michael Lenz and Joseph Yelk who made technical contributions to the experiment. This research is supported by the U.S. Department of Energy under Contract Nos. DE-AC02-76CH00016 and DE-AC02-76ER03075.

REFERENCES

1. P. Bloch, et al., Phys. Lett. 56B, 201 (1975); N.J. Baker, et al., Phys. Rev. Lett. 59, 2832 (1987).
2. J.F. Donoghue, B.R. Holstein, and G. Valencia, Phys. Rev. D35, 2769 (1987); G. Ecker, A. Pich, and E. deRafael, Nucl. Phys. B291, 692 (1987), G. Ecker, A. Pich, and E. deRafael, Nucl. Phys. B303, 665 (1988).
3. The ratio of the K^0_L/K^+ lifetimes is 4.2. K^0_L is a coherent sum of $K^0-\bar{K}^0$ which has the same CP as the final state $\pi^0 + \text{scalar}$. K^0_S has opposite CP.
4. L.J. Hall and L.J. Randall, Nucl. Phys. B274, 157 (1986).
5. A.S. Carroll, et al., Phys. Rev. Lett. 44, 525 (1980).
6. L.M. Sehgal, Phys. Rev. 183, 1511 (1969), M. Holder, Annals of New York Academy of Science 518, 140 (1987).
7. H.B. Greenlee, et al., Phys Rev. Lett. 60, 893 (1988).
8. An event is rejected if there is an extra space point in the A drift chamber within 6 mm of a line extrapolated from the decay vertex to an extra space point in the B drift chamber.
9. L. Bergström, Z. Phys. C20, 135 (1983).
10. M. Mannelli, et al., in Proceedings of the 23rd Recontres de Moriond, Les Arcs, France, March 6-13, 1988 (to be published).

The additional hits in the A and B drift chambers were not consistent with originating at the decay vertex within the accuracy of the drift chamber measurements. However, if their momenta were about 170 MeV/c and 200 MeV/c, the trajectories were consistent with originating at the vertex when the effects of multiple scattering in the vacuum window

and magnetic curvature in the small fringe field between the A and B chambers is taken into consideration. These particles would have curled in the spectrometer field and would not have been observed in the C and D drift chambers. The effective mass combinations are then $m(\gamma_1 e^+ e^-_1) = 125 \text{ MeV}/c^2$, $m(\gamma_2 e^+ e^-_2) = 145 \text{ MeV}/c^2$, and $m(\gamma_1 \gamma_2 e^+ e^-_1 e^-_2) = 497 \text{ MeV}/c^2$, consistent with the π^0 and K^0 masses respectively. The lead glass E/p for the high energy positron and electron were 1.01 and 1.05 respectively. We calculate the probability of observing a $\pi^0 \pi^0$ decay with both π^0 's undergoing Dalitz decay such that a $\gamma \gamma e^+ e^-$ effective mass combination is $480 \text{ MeV}/c^2$ or higher is less than 1%.

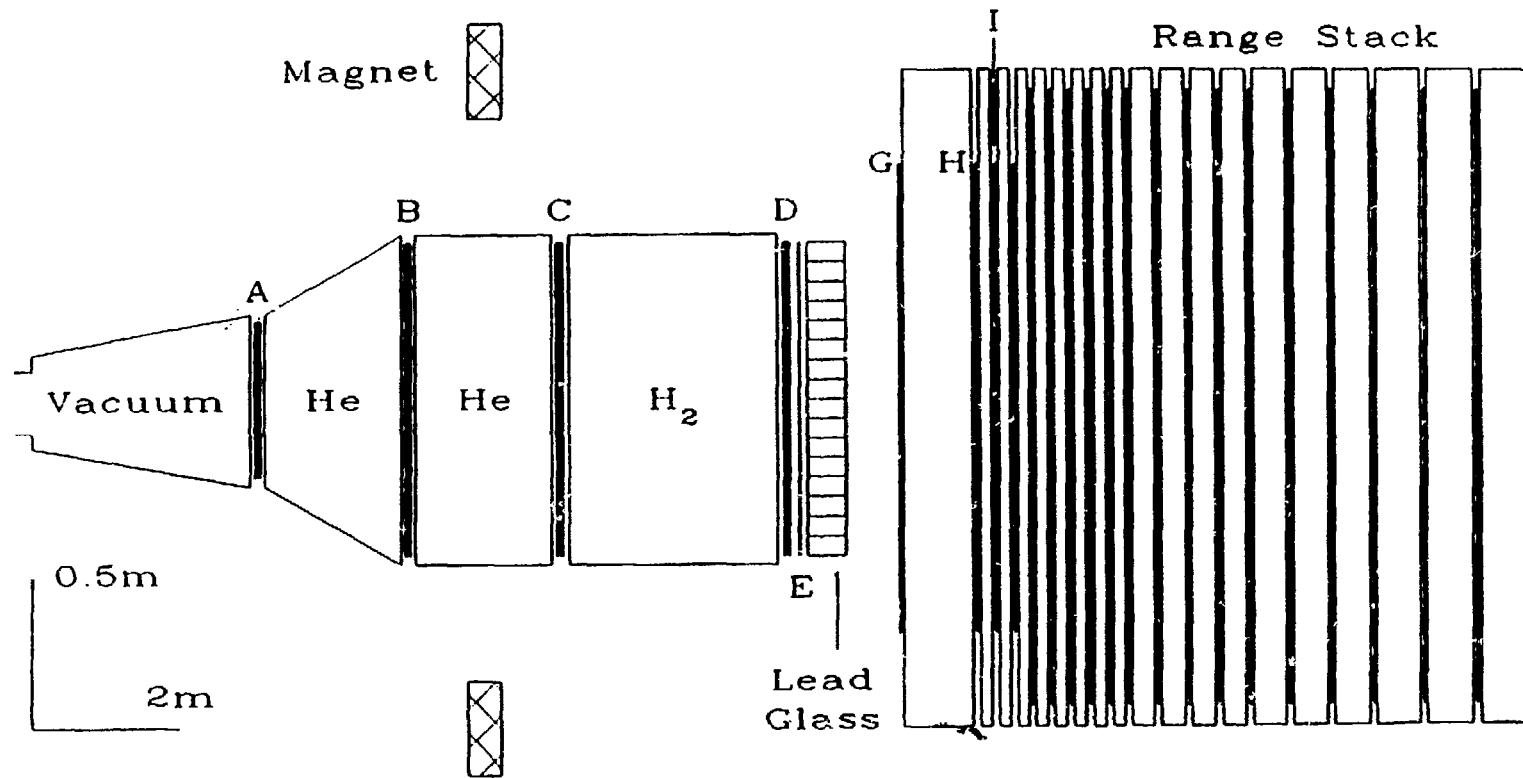


Fig. 1. Plan view of the E780 detector. Note the different horizontal and vertical scales.

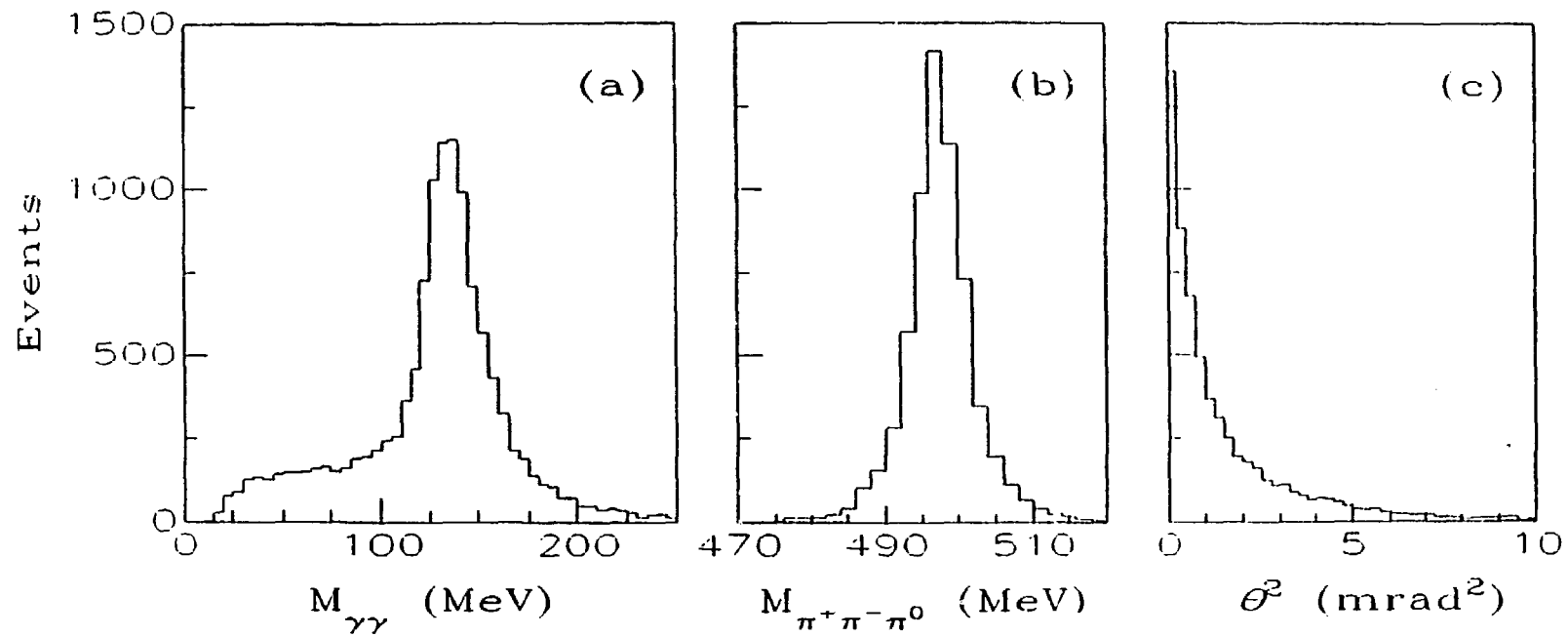


Fig. 2. Distributions of (a) $\gamma\gamma$ effective mass, (b) $\pi^+\pi^-\pi^0$ effective mass for events with $\theta^2 < 10 \text{ mrad}^2$, and (c) the square of the target reconstruction angle for events within $12.5 \text{ MeV}/c^2$ of the K mass.

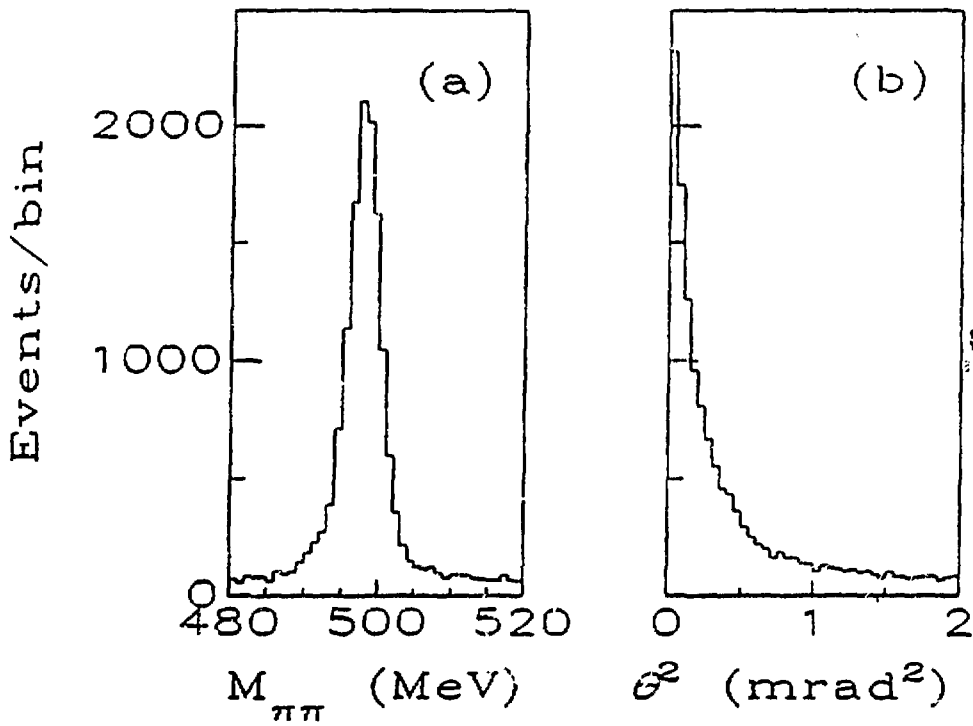


Fig. 3. Distributions of (a) the $\pi^+\pi^-$ invariant mass for inbending events with $\theta^2 < 1.5 \text{ mrad}^2$ and (b) the square of the target reconstruction angle for events within three sigma of the K mass.

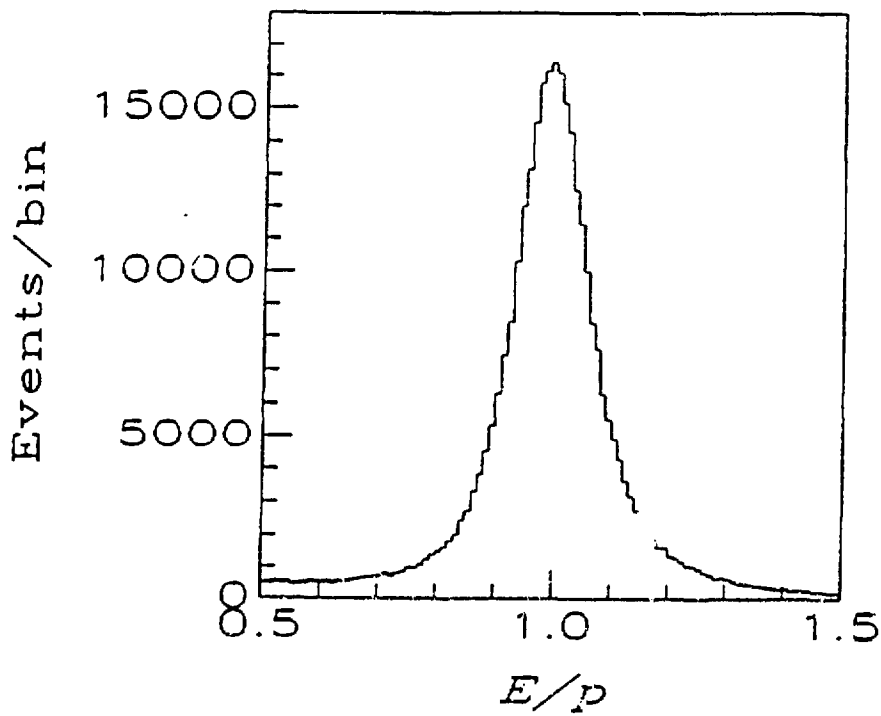


Fig. 4. Distribution of energy measured in the lead glass divided by momentum measured in the magnetic spectrometer for electrons from K_{e3} decays.

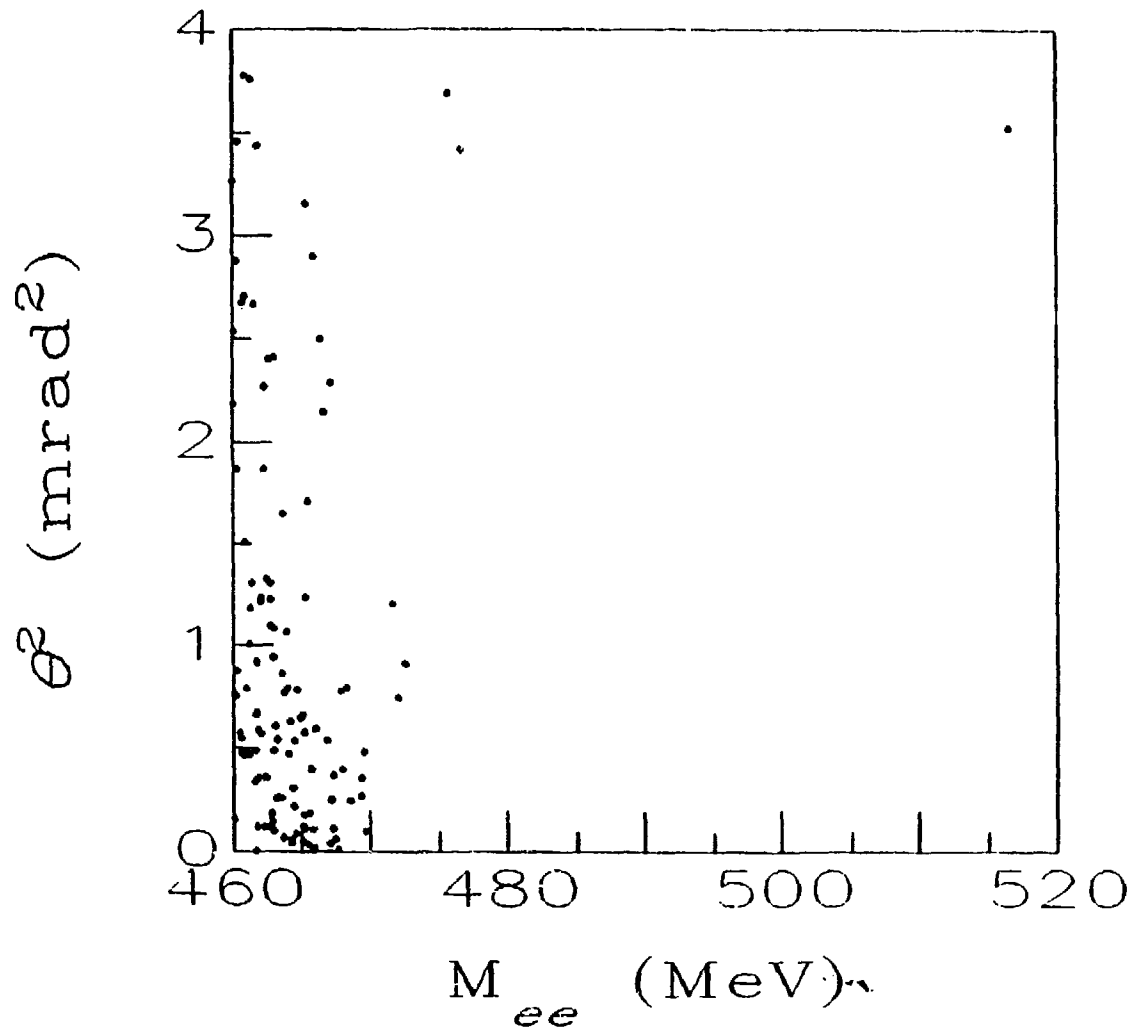


Fig. 5. Scatter plot of the e^+e^- effective mass vs. the square of the target reconstruction angle.

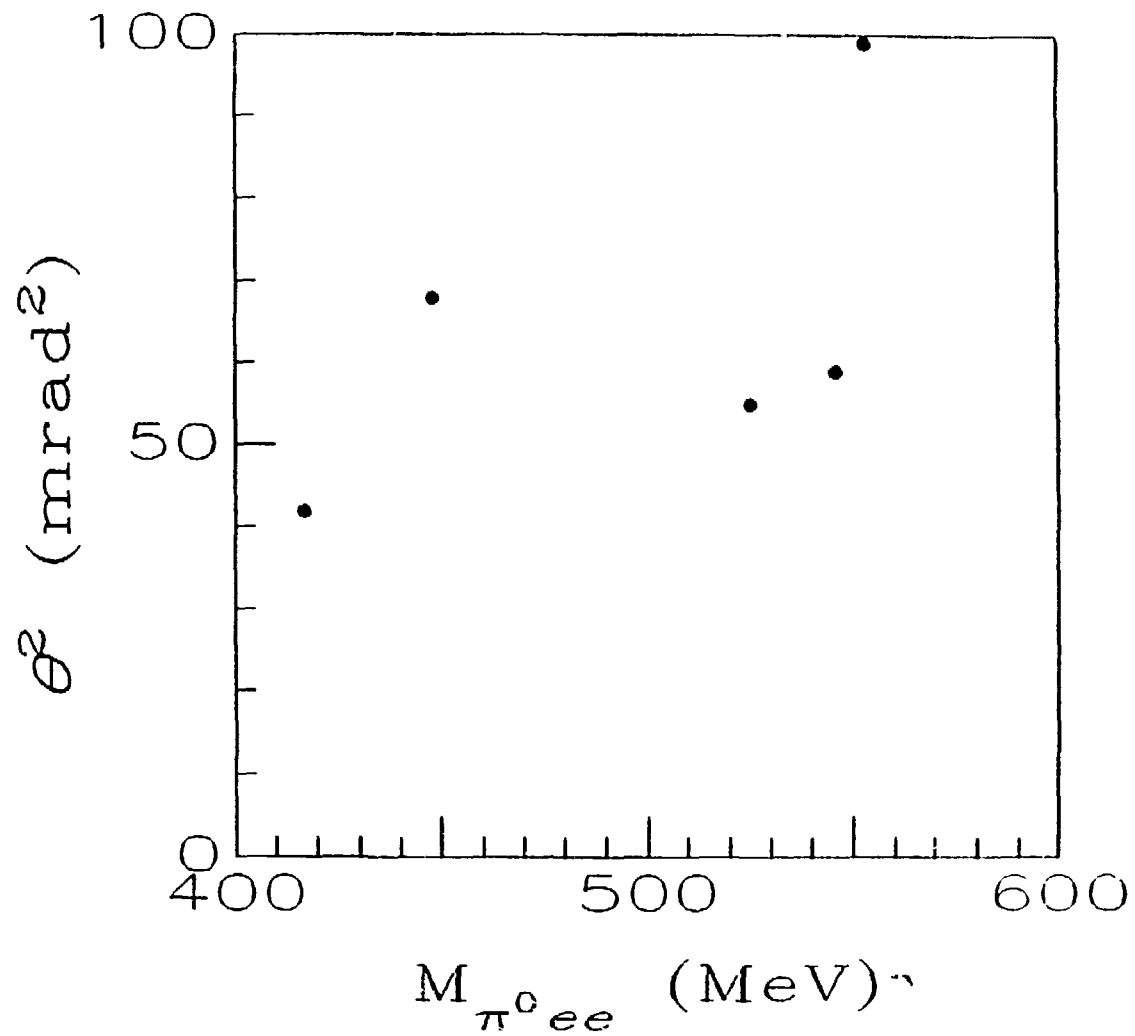


Fig. 6. Scatter plot of the $\pi^0 e^+ e^-$ effective mass vs. the square of the target reconstruction angle.

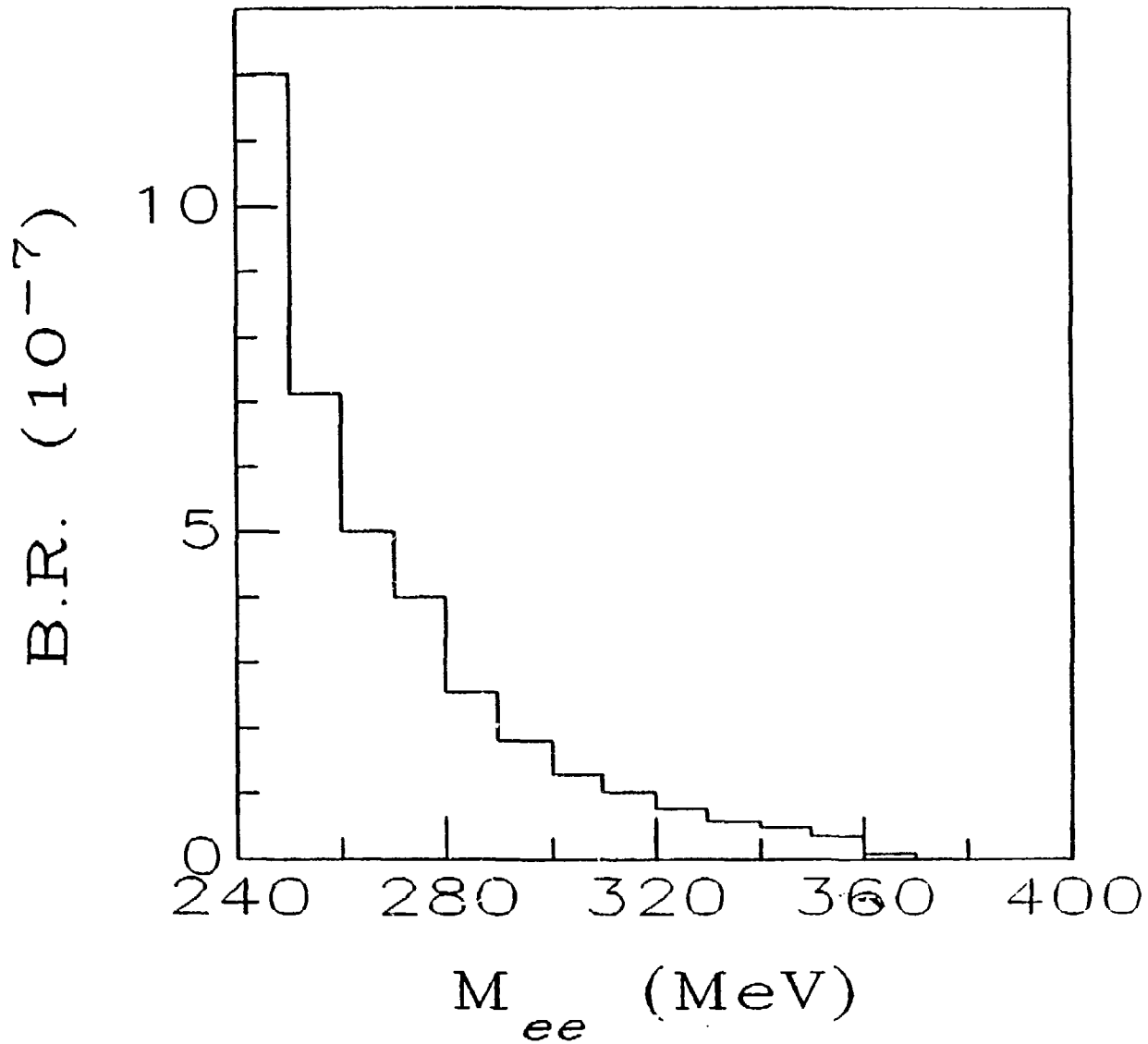


Fig. 7. 90% confidence level limits on $K_L^0 \rightarrow \pi^0 e^+ e^-$ as a function of e^+e^- effective mass.

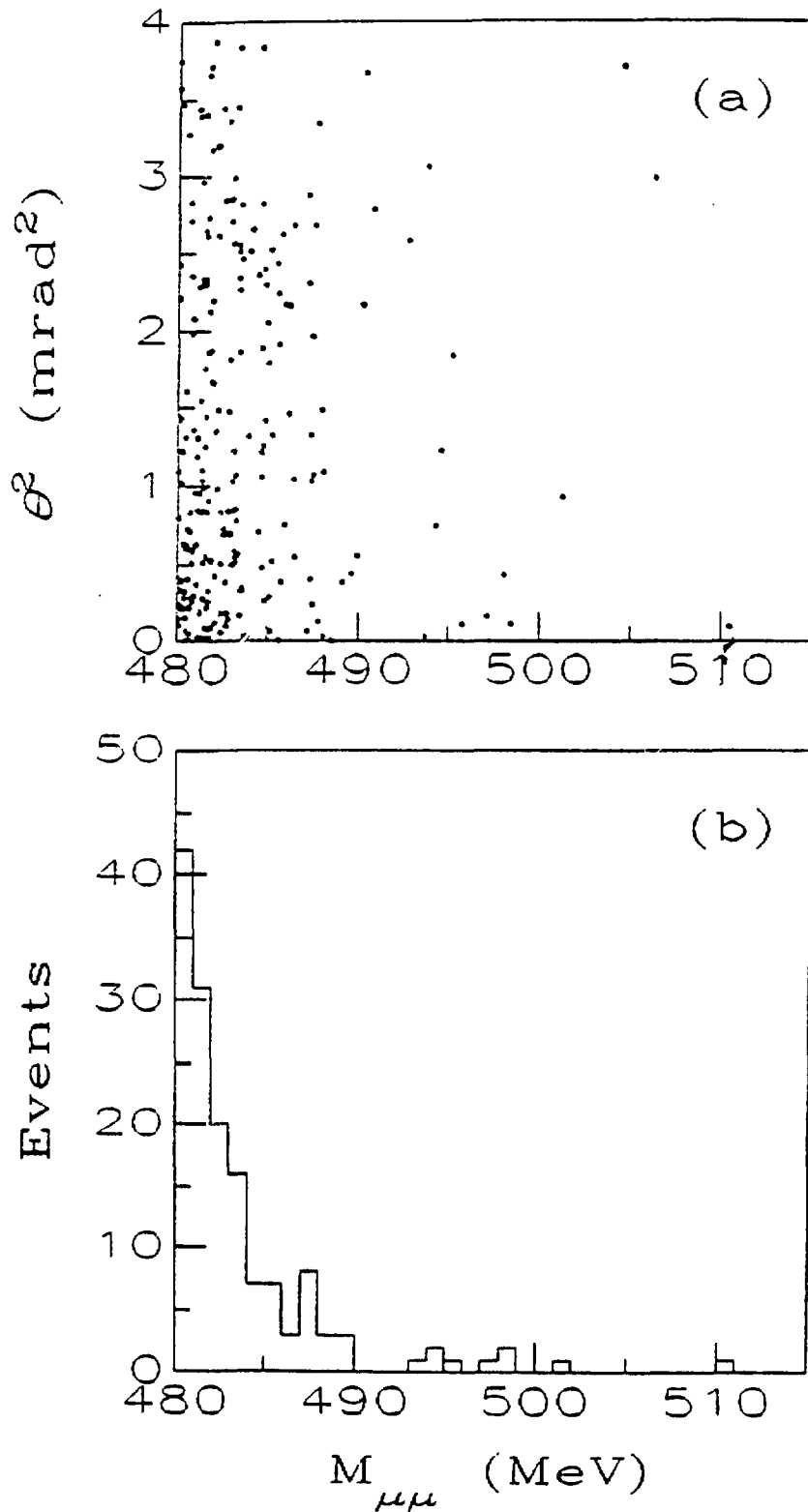


Fig. 8. a) Scatter plot of $\mu^+\mu^-$ effective mass vs. θ^2 .
 b) Distribution of $\mu^+\mu^-$ effective mass for events with $\theta^2 < 1.5 \text{ mrad}^2$.

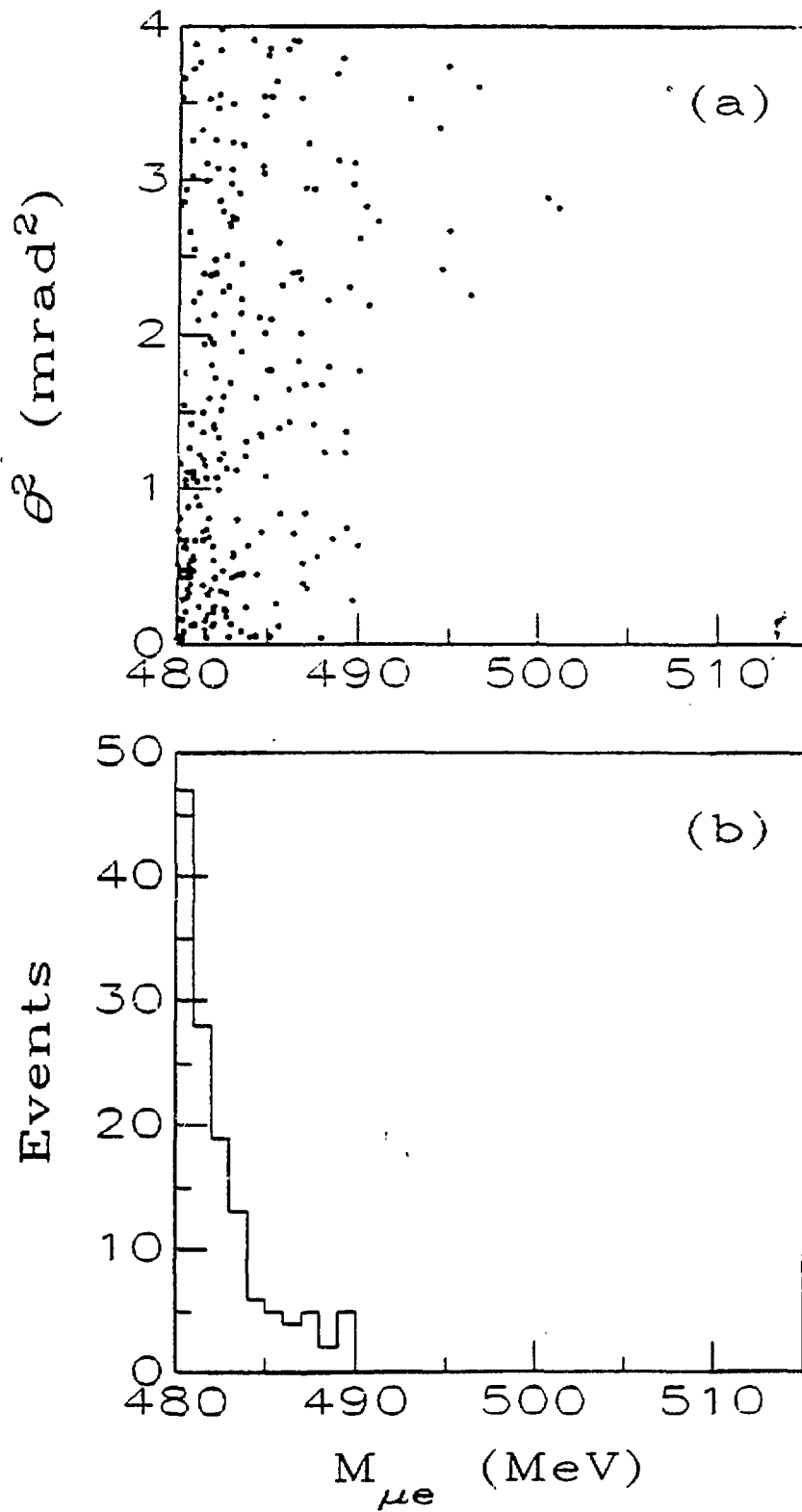


Fig. 9. a) Scatter plot of μ^+e^- effective mass vs. θ^2 .
 b) Distribution of μ^+e^- effective mass for events with $\theta^2 < 1.5 \text{ mrad}^2$.